Received: 14 July 2023 | Accepted: 17 August 2023

DOI: 10.1111/cts.13644

ARTICLE

Study of the ketohexokinase inhibitor PF-06835919 as a clinical cytochrome P450 3A inducer: Integrated use of oral midazolam and liquid biopsy

Ruolun Qiu[1] | **Kari Fonseca**[1] | **Arthur Bergman**[1] | **Jian Lin**[2] | **David Tess**[1] | **Lauren Newman**[3] | **Alia Fahmy**[3] | **Zivile Useckaite**[3] | **Andrew Rowland**[3] | **Manoli Vourvahis**[4] | **David Rodrigues**[2]

[1]Pfizer Inc, Cambridge, Massachusetts, USA

[2]Pfizer Inc, Groton, Connecticut, USA

[3]Flinders University, Adelaide, South Australia, Australia

[4]Pfizer Inc, New York, New York, USA

Correspondence
Ruolun Qiu, Pfizer Inc, 610 N. Main Street, 1st Floor 104, Cambridge, MA 02139, USA.
Email: ruolun.qiu@pfizer.com

Funding information
Pfizer Inc

Abstract

PF-06835919, a ketohexokinase inhibitor, presented as an inducer of cytochrome P450 3A4 (CYP3A4) in vitro (human primary hepatocytes), and static mechanistic modeling exercises predicted significant induction in vivo (oral midazolam area under the plasma concentration-time curve [AUC] ratio [AUCR] = 0.23–0.79). Therefore, a drug–drug interaction study was conducted to evaluate the effect of multiple doses of PF-06835919 (300 mg once daily × 10 days; $N = 10$ healthy participants) on the pharmacokinetics of a single oral midazolam 7.5 mg dose. The adjusted geometric means for midazolam AUC and its maximal plasma concentration were similar following co-administration with PF-06835919 (vs. midazolam administration alone), with ratios of the adjusted geometric means (90% confidence interval [CI]) of 97.6% (90% CI: 79.9%–119%) and 98.9% (90% CI: 76.4%–128%), respectively, suggesting there was minimal effect of PF-06835919 on midazolam pharmacokinetics. Lack of CYP3A4 induction was confirmed after the preparation of subject plasma-derived small extracellular vesicles (sEVs) and conducting proteomic and activity (midazolam 1′-hydroxylase) analysis. Consistent with the midazolam AUCR observed, the CYP3A4 protein expression fold-induction (geometric mean, 90% CI) was low in liver (0.9, 90% CI: 0.7–1.2) and non-liver (0.9, 90% CI: 0.7-1.2) sEVs (predicted AUCR = 1.0, 90% CI: 0.9–1.2). Likewise, minimal induction of CYP3A4 activity (geometric mean, 90% CI) in both liver (1.1, 90% CI: 0.9–1.3) and non-liver (0.9, 90% CI: 0.5-1.5) sEVs was evident (predicted AUCR = 0.9, 90% CI: 0.6-1.4). The results showcase the integrated use of an oral CYP3A probe (midazolam) and plasma-derived sEVs to assess a drug candidate as inducer.

ClinicalTrials.gov identifier: NCT03916406.

Study Highlights

WHAT IS THE CURRENT KNOWLEDGE ON THE TOPIC?

In vitro, ketohexokinase inhibitor PF-06835919 behaved as a cytochrome P450 3A4 (CYP3A4) inducer. Plasma-derived tissue-specific small extracellular vesicles (sEVs) have successfully evaluated CYP3A induction following the administration of an inducer to enable prediction of midazolam area under the plasma concentration-time curve ratio (AUCR) in clinical studies.

WHAT QUESTION DID THIS STUDY ADDRESS?

Is it possible to clinically deploy oral midazolam and plasma-derived sEVs to assess CYP3A4 induction by a compound, such as PF-06835919? Furthermore, can the sEV data be used to predict the AUCR of midazolam?

WHAT DOES THIS STUDY ADD TO OUR KNOWLEDGE?

It is possible to utilize oral midazolam, jointly with profiled plasma-derived sEVs, to successfully study the induction of CYP3A4. In the case of PF-06835919, both approaches presented it as a false-positive non-inducer compared to rifampicin and modafinil.

HOW MIGHT THIS CHANGE CLINICAL PHARMACOLOGY OR TRANSLATIONAL SCIENCE?

It is possible to obtain plasma-derived sEVs from subjects enrolled in a standard multiple ascending dose phase I study and profile them for CYP3A4 expression and activity. In doing so, CYP3A4 induction can be assessed without the need for a formal drug interaction study.

INTRODUCTION

Increased fructose consumption and its subsequent metabolism have been implicated in metabolic disorders, such as nonalcoholic fatty liver disease (NAFLD) and steatohepatitis and insulin resistance.[1–3] Ketohexokinase (KHK) catalyzes the conversion of fructose and adenosine triphosphate to fructose-1-phosphate and adenosine diphosphate, the first committed step in fructose metabolism.[4] Inhibition of KHK has been found to offer protection against fatty liver disease in fructose-fed mice, and so represents a potential therapeutic target for treating patients with NAFLD.[5] Preclinical and clinical studies have shown that PF-06835919, a potent, reversible inhibitor of human KHK,[6] can reduce cardiovascular risk factors in rats fed with a typical American diet and can decrease hepatic fructose metabolism in both rats and healthy humans while increasing levels of fructose in plasma and urine.[7,8]

PF-06835919 is an orally available small molecule; in vitro it presents high passive permeability and is not a P-glycoprotein substrate. However, PF-06835919 is a substrate for the efflux transporter breast cancer resistance protein and the hepatic uptake transporters organic anion transporter 2 and organic anion transporting polypeptide 1B1. The clearance of PF-06835919 is proposed to be mediated by hepatic uptake primarily by the former, with a minor contribution from the latter, followed by subsequent metabolism involving both cytochrome P450s and UDP-glucuronosyltransferases.[9] In addition, in vitro studies demonstrated that PF-06835919 is a cytochrome P450 3A4 (CYP3A4) inducer. Based on the in vitro induction data and the projected clinical dose prior to first-in-human dosing, the CYP3A drug–drug interaction (DDI) liability for PF-06835919 was assessed using static mechanistic modeling which predicted a potential risk for clinical induction. Therefore, a phase I clinical study was conducted to assess the potential of PF-06835919 to induce CYP3A metabolism using oral midazolam, a CYP3A4/5 probe substrate.[10]

More recently, it has been possible to study CYP3A4 induction using tissue-specific plasma (serum)-derived small extracellular vesicles (sEVs).[11–14] Such an approach is possible because various sEVs are shed into the blood and contain cargo that is representative of their tissue of origin. Therefore, it is feasible to obtain plasma from subjects and assess CYP3A4 protein expression and activity changes (pre- vs. post-inducer) in global (all tissues) and immunocaptured (anti-asialoglycoprotein receptor 1-positive) liver sEVs. This approach has already been successfully deployed following the administration of a strong (rifampicin 600 mg) and weak/moderate (modafinil 400 mg) inducer, which enabled the prediction of victim drug (e.g., midazolam)

area under the plasma concentration-time curve (AUC) ratio (AUCR, $AUC_{+inducer}/AUC_{-reference}$) observed in clinical studies.[13,14]

In this paper, we describe a phase I clinical study conducted to evaluate the CYP3A induction potential of PF-06835919 with healthy adult participants. In addition, preparations of plasma-derived sEVs were deployed as liquid biopsy to support an ad hoc analysis to confirm the results obtained with the CYP3A probe drug midazolam.

METHODS

In vitro human hepatocyte study and drug–drug interaction prediction

The detailed methods for the human hepatocyte experiment to assess CYP3A induction potential, in vitro data analyses, and prediction of in vivo DDIs are described in the Supplementary Methods ("CYP3A induction in human hepatocytes," "In vitro induction data analysis," "In vitro induction slope calibration," and "Predicting the magnitude of DDIs" subsections in Data S1).

Compound and reagents are listed in the Supplementary Methods ("Compound and reagents" subsection in Data S1).

Clinical study design

C1061016 was a phase I, randomized, two-way crossover, open-label study in healthy participants that examined the effect of repeated dosing of PF-06835919 on the pharmacokinetics (PKs) of a single oral dose of midazolam (NCT03916406). Participants were randomized to one of two treatment sequences. Treatment sequence one consisted of a single 7.5 mg oral dose of midazolam alone in period one followed by a once-daily dose of PF-06835919 300 mg for 9 days followed by a single oral dose of PF-06835919 300 mg and a 7.5 mg oral dose of midazolam on day 10 in period two. Treatment sequence two was a once-daily dose of PF-06835919 300 mg for 9 days followed by a single oral dose of PF-06835919 300 mg and a 7.5 mg oral dose of midazolam on day 10 in period one followed by a single oral dose of PF-06835919 300 mg alone in period two. PF-06835919 was administered as 100 mg tablets, whereas midazolam was administered as a commercially available oral midazolam solution (2 mg/mL). There was a minimum 10-day washout between the two treatment periods for each sequence. A total of 10 healthy male and/or female participants were enrolled in this study, with five participants in each treatment sequence.

Participants were confined to the clinical research unit for a total of 3 days and 2 nights for the treatment period with midazolam administered alone and a total of 12 days and 11 nights for the treatment period when PF-06835919 was co-administered with midazolam. The study was conducted at the Pfizer Clinical Research Unit in Brussels, Belgium.

PK assessments

Blood samples for midazolam plasma concentration were collected at: predose, 0.5, 1, 2, 4, 6, 8, 10, 12, 16, and 24 h after each midazolam dose. Plasma samples were analyzed for midazolam concentrations at Covance Inc (Indianapolis, USA), using a validated, sensitive, and specific liquid chromatography tandem mass spectrometric method. Plasma specimens were stored at ~−20°C until analysis and assayed within the 150 days of established stability data generated during validation. The lower limit of quantification (LLOQ) for midazolam was 0.100 ng/mL.

The concentration population was defined as all enrolled, treated subjects who had at least one measurable midazolam concentration. The PK parameter population was defined as all enrolled, treated subjects who had at least one of the PK parameters of interest measured.

Plasma midazolam PK parameters were calculated using noncompartmental analysis of concentration-time data. Samples below the LLOQ were set to 0 ng/mL for PK analysis. Midazolam PK parameters included: maximum plasma concentration (C_{max}), observed directly from data; AUC from time 0 to the time of the last quantifiable concentration (AUC_{last}), determined by linear/log trapezoidal rule; AUC from time 0 extrapolated to infinite time (AUC_{inf}), determined by $AUC_{last}+(C_{last}*/k_{el})$ where $C_{last}*$ was the predicted plasma concentration at the last quantifiable time point estimated from the log-linear regression analysis; time at C_{max} (T_{max}), observed directly from the data; terminal elimination half-life ($t_{½}$), determined by $Log_e(2)/k_{el}$, where k_{el} is the terminal phase rate constant calculated by a linear regression of the log-linear concentration-time curve.

Safety assessments

The safety and tolerability of PF-06835919 when co-administered with a single, oral dose of midazolam were evaluated in the study. All subjects who received at least one dose of study medication were included in the safety analyses. Safety measures included an assessment of adverse events (AEs; spontaneous and solicited), blood and urine laboratory tests, vital signs, and

electrocardiograms. Serious AEs (SAEs) were defined as any that resulted in death, were life-threatening, required inpatient hospitalization or prolongation of existing hospitalization, resulted in persistent or significant disability/incapacity, or resulted in congenital anomaly/birth defect. All treatment-emergent AEs (TEAEs) and their severity and potential causality were recorded by investigators from the time the subject had taken at least one dose of study medication through their last follow-up.

Statistical analysis

The PK parameters of midazolam were summarized descriptively by treatment. In addition, natural log-transformed AUC_{inf} of midazolam was analyzed using a mixed-effect model with sequence, period, and treatment as fixed effects and participant within sequence as a random effect. Estimates of the adjusted mean differences (test/reference) and corresponding 90% confidence intervals (CIs) were obtained from the model. The adjusted mean differences and 90% CIs for the differences were exponentiated to provide estimates of the ratio of adjusted geometric means (test/reference) and 90% CIs for the ratios. Midazolam alone was the reference treatment, whereas midazolam co-administered with PF-06835919 was the test treatment.

Ethical principles

The clinical study was conducted in compliance with the ethical principles of the Declaration of Helsinki and the International Conference on Harmonisation Good Clinical Practice guidelines. The protocol was approved by the independent ethics committee at the investigational center. All subjects provided informed consent.

sEV study

Methods for the preparation of plasma-derived sEVs and analysis of CYP3A4 protein expression and activity (midazolam 1′-hydroxylase), as well as the prediction of midazolam AUCR, are described in the Supplementary Methods ("Isolation of plasma-derived small extracellular vesicles (sEVs)," "sEVs peptide digestion and proteomic analysis of cytochrome P450 3A4 (CYP3A4)," "Measurement of midazolam (MDZ) hydroxylase activity in global and liver sEVs," and "Predicting MDZ area under the plasma concentration-time curve ratio (AUCR) based on plasma-derived sEVs CYP3A4 activity and proteomic data" subsections in Data S1). For the prediction of midazolam AUCR based on sEVs CYP3A4 expression changes, data from two published studies (rifampicin and modafinil) were also leveraged.[13,14]

RESULTS

CYP3A induction in human hepatocytes

The induction of CYP3A messenger ribonucleic acid (mRNA) and enzyme activity (midazolam 1′-hydroxylase) by PF-06835919 was examined in vitro using cryopreserved plated human hepatocytes. Treatment with PF-06835919, at concentrations ranging from 0.5–200 μM, resulted in concentration-dependent increases in both CYP3A mRNA and activity (midazolam 1′-hydroxylase) in all three lots of hepatocytes examined (Figure 1). No cytotoxicity was observed with PF-06835919 treatment. The induction parameters were estimated using sigmoid and linear fits, and the preferred model was selected using the built-in extra sum-of-squares *F*-test. The best fit of the fold-induction mRNA response in two lots of hepatocytes, and that of CYP3A activity in hepatocyte lot HC7-4, was obtained using a linear model.

In vitro DDI risk assessment

The clinical relevance of in vitro induction was assessed by mechanistic static models recommended by the US Food and Drug Administration (FDA)[10] and an internal Pfizer (PFE) mechanistic static model, and predictions for both models are summarized in Table 1. The FDA mechanistic static model uses a rapid absorption rate constant and essentially assumes that the concentration of the perpetrator drug in the enterocyte is equal to the concentration of the total dose dissolved in the intestinal lumen fluids, coupled with a maximal inducer unbound concentration in the portal vein ($I_{max,inlet,u}$), for the prediction of the hepatic interaction (AUCR = 0.23). Based on exposure-response analysis of rifampicin, CYP3A4 induction is driven by AUC. Therefore, the average free drug concentration in plasma is currently used in the PFE internal mechanistic model for induction prediction. Using the calibrated induction slope, the internal mechanistic model predicted approximately similar increases (1.2-fold) in active CYP3A4 in both gut and liver. Additional consideration of two estimated hepatic unbound partition coefficients (1 and 10) for PF-06835919, rendered predicted midazolam AUCR values of 0.34 to 0.79 (Table 1).

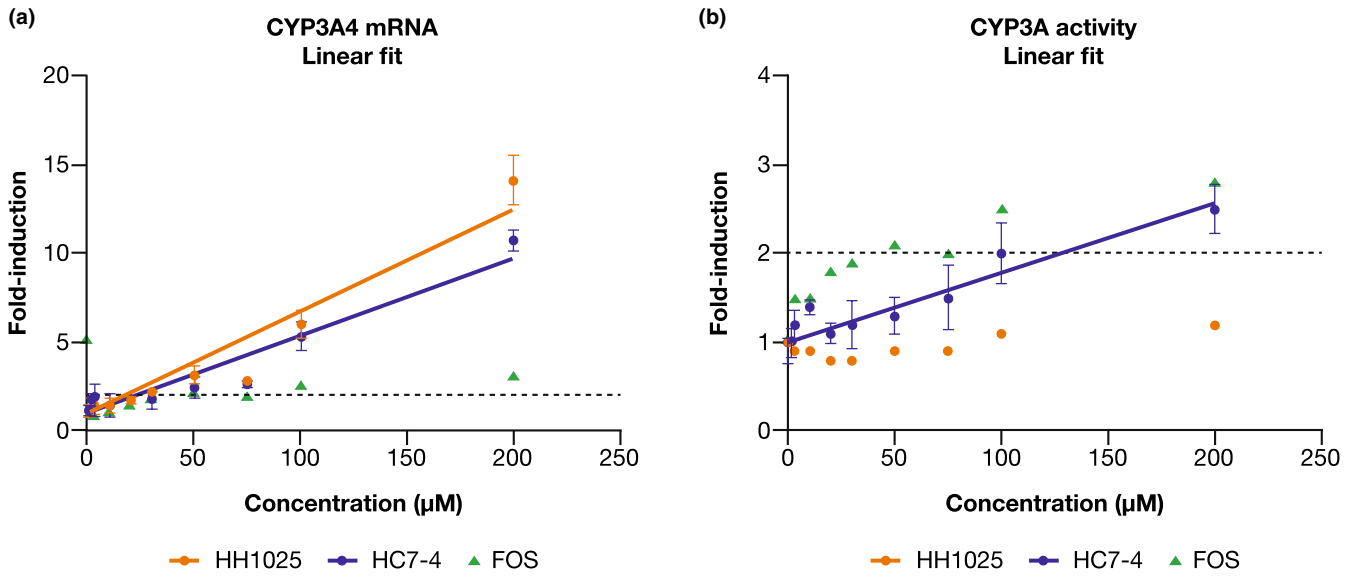

FIGURE 1 Summary of fold-induction of (a) CYP3A mRNA activity and (b) CYP3A enzyme activity in three different lots of plated cryopreserved human hepatocytes treated with PF-06835919. Fold-induction in each lot of hepatocytes was fitted to a linear model. Dashed lines at two-fold represent the threshold for induction. CYP3A4, cytochrome P450 3A4; mRNA, messenger ribonucleic acid.

TABLE 1 Static mechanistic modeling predictions of CYP3A induction.

Model	$Kp_{,uu}$	I_g (μM)	C_g	I_h (μM)	C_h	Predicted AUCR[a]
FDA	1	44.5	5.45	5.5	1.55	0.23
PFE	10	2.01	1.20	17.6	2.76	0.34
	1	2.01	1.20	1.76	1.18	0.79

Abbreviations: AUCR, area under the plasma concentration-time curve ratio; C_g, induction effect in the intestine; C_h, induction effect in the liver; CYP3A4, cytochrome P450 3A4; FDA, US Food and Drug Administration; I_g, concentration in the gut; I_h, concentration in the liver; $Kp_{,uu}$, unbound partition coefficient; PFE, Pfizer.

[a]See the Supplementary Methods, "Predicting the magnitude of drug-drug interaction (DDI)" subsection (AUCR) in Data S1.

Participants

In total, 10 healthy adult participants were assigned to treatment in this study, five participants for each sequence. All participants were treated and completed the study. Demographics for treated subjects are summarized in Table 2. All participants were White men. The mean age for all treated participants was 38.7 (range: 25–48) years. The mean body weight and body mass index were 77.0 (range: 62.4–92.2) kg and 25.2 (range: 22.8–29.0) kg/m^2, respectively.

TABLE 2 Demographics of healthy participants in study C1061016.

	All subjects
Male, *N* (%)	10 (100)
Mean age (range), years	38.7 (25.0–48.0)
Race, *N* (%)	
White	10 (100)
Mean body weight (range), kg	77.0 (62.4–92.2)
Mean BMI (range), kg/m^2	25.2 (22.8–29.0)

Abbreviation: BMI, body mass index.

Midazolam PK

Median midazolam plasma concentration-time profiles administered with or without multiple doses of PF-06835919 are shown in Figure 2. PK parameters and accompanying adjusted geometric means for midazolam in the presence and absence of PF-06835919 are listed in Table 3.

Median plasma midazolam concentrations were similar following multiple doses of PF-06835919 compared to those observed for midazolam administered alone. Midazolam T_{max} values were similar between treatment

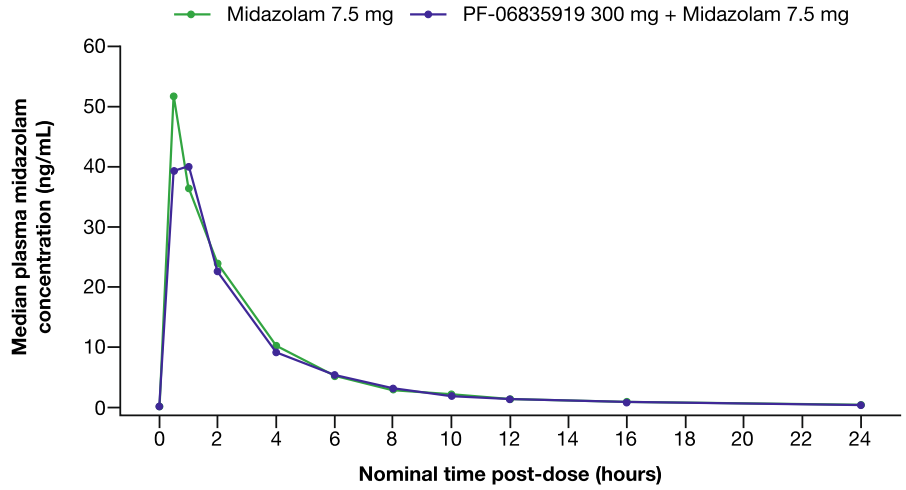

FIGURE 2 Median midazolam plasma concentration-time profiles after a single oral dose of midazolam 7.5 mg with or without PF-06835919 300 mg once daily.

TABLE 3 Descriptive summary of plasma midazolam PK parameters with or without PF-06835919.

Parameter (unit)	Midazolam 7.5 mg	PF-06835919 300 mg + midazolam 7.5 mg
N	10	10
AUC_{inf} (ng.h/mL)	130.8 (35)	127.6 (60)
AUC_{last} (ng.h/mL)	127.9 (34)	124.7 (58)
C_{max} (ng/mL)	43.97 (44)	43.49 (48)
T_{max} (h)	0.51 (0.50–2.00)	0.50 (0.50–1.03)
$t_{1/2}$ (h)	5.267 ± 1.885	4.986 ± 1.551

Abbreviations: AUC, area under the plasma concentration-time curve; AUC_{inf}, AUC from time 0 extrapolated to infinite time; AUC_{last}, AUC from time 0 to the time of the last quantifiable concentration; C_{max}, maximum plasma concentration; PK, pharmacokinetics; $t_{1/2}$, terminal elimination half-life; T_{max}, time at C_{max}.

periods (median T_{max} of 0.5 h) and its plasma concentration declined in a monophasic manner with a similar mean $t_{½}$ observed between the treatments (5.3 h for midazolam administered alone vs. 4.9 h when administered with multiple doses of PF-06835919). The adjusted geometric means for midazolam plasma AUC_{inf}, AUC_{last}, and C_{max} were similar following co-administration with multiple doses of PF-06835919 as compared to midazolam administration alone with the ratios of the adjusted geometric means (90% CI) of 97.6% (90% CI: 79.9%–119%), 97.4% (90% CI: 80.2%–118%), and 98.9% (90% CI: 76.4%–128%), respectively, suggesting that there was minimal effect of PF-06835919 on single-dose midazolam PK.

Safety

All treated participants were evaluated for AEs. In general, repeated doses of PF-06835919 300 mg for 9 days followed by a single oral dose of PF-06835919 300 mg co-administered with midazolam 7.5 mg was well-tolerated in healthy participants with no deaths, SAEs, severe AEs, discontinuation, or dose reductions due to AEs reported in this study. The most frequently reported TEAE was somnolence, which occurred in six participants with midazolam alone and six following co-administration of midazolam and PF-06835919, and consistent with the established product characteristics of midazolam. Treatment with PF-06835919 alone was associated with numerically lower TEAEs as compared with midazolam alone, or co-administration. The majority of TEAEs reported were considered treatment-related and mild in severity.

sEV study results

Global and liver sEVs were prepared from the plasma of study subjects pre- and postdosing of PF-06835919 for 10 days. Thereafter, the sEVs were subjected to CYP3A4 proteomics analysis and measurement of midazolam 1′-hydroxylase activity. The individual subject data for global, liver, and non-liver (global minus liver) sEVs are summarized in Table S1. Consistent with the midazolam AUCR reported in the clinical study, the CYP3A4 protein expression fold-induction (geometric mean, 90% CI) was low in liver (0.9, 90% CI: 0.7–1.2) and non-liver (0.9. 90% CI: 0.7-1.2) sEVs (Table 4). Minimal induction was also observed for CYP3A4 activity in both liver (geometric mean fold-increase = 1.1, 90% CI: 0.9–1.3) and non-liver

(geometric mean fold-increase = 0.9, 90% CI: 0.5-1.5) sEVs. In the case of the latter, the data were more variable across subjects. Importantly, CYP3A4 protein expression was highly and significantly correlated ($r \geq 0.820$, $p \leq 0.0006$) with midazolam 1′-hydroxylase activity in global, liver, and non-liver sEVs (Figure 3a–c).

Using the sEV CYP3A4 protein and activity data, it was possible to predict the midazolam AUCR following PF-06835919 (Table 4). In this instance, it was assumed that *CYP3A4* and *CYP3A5* genotype did not impact the analysis and that the midazolam fraction surviving gut first pass (f_g) and fraction metabolized by CYP3A4 ($f_{m,CYP3A4}$) was 0.51 and 0.9, respectively, to support integration with previously published modafinil and rifampicin data.[13,14] Such model inputs were different from those used to support the above described in vitro human hepatocyte-based predictions to midazolam AUCR (Supplementary Methods in Data S1; $f_{m,CYP3A4} = 0.96$; $f_g = 0.58$). Therefore, sEV-based predictions of midazolam AUCR were repeated with these different $f_{m,CYP3A4}$ and f_g inputs with minimal impact on the outcome (Pfizer Inc data on file).

Of note, all subjects (except subject 5 genotyped *CYP3A4*1B/*1B* and subject 8 genotyped *CYP3A4*1/*1B*) were genotyped *CYP3A4*1/*1* (Linda Wood, Pfizer, personal communication). In addition, all subjects were CYP3A5 non-expressers (*CYP3A5*3/*3*), except for subject 5 (*CYP3A5*1/*7*), subject 7 (*CYP3A5*1/*3*), and subject 8 (*CYP3A5*1/*3*). As shown in Table 4, the predicted geometric mean AUCR (90% CI) for midazolam was 1.0 (90% CI: 0.9-1.2) and 0.9 (90% CI: 0.6-1.4), based on sEV CYP3A4 protein expression and activity changes, respectively. Based on the sEV CYP3A4 expression and activity data described, it was possible to correctly classify PF-06835919 as a non-inducer compared to rifampicin and modafinil (Figure 3d).

DISCUSSION

In vitro hepatocyte studies suggested the potential for PF-06835919 to induce CYP3A with high risk at clinically relevant exposures (Table 1). Therefore, the purpose of the described clinical study was to evaluate the potential of PF-06835919 to induce the metabolism of a sensitive CYP3A substrate (midazolam). The results of this study would provide information regarding the possible risks of co-administration of CYP3A substrates with PF-06835919 in future clinical trials. The study results suggested that there was a minimal effect of repeated dosing of PF-06835919 on the exposure of oral midazolam, as the ratio of the adjusted geometric mean (90% CI) of AUC_{inf} and C_{max} for midazolam following co-administration with multiple doses of PF-06835919,

TABLE 4 PF-06835919 as a CYP3A4 inducer.

	Fold-change CYP3A4 protein expression (day 10/day 1)[a]		Fold-change CYP3A4 activity (day 10/day 1)[a,b]		Predicted midazolam AUCR[c]	
Subject	Liver sEVs	Non-liver sEVs	Liver sEVs	Non-liver sEVs	sEV CYP3A4 protein	sEV CYP3A4 activity
1	0.3	ND	1.0	1.6	ND	0.8
2	0.8	0.6	1.1	ND	1.5	ND
3	1.0	ND	1.0	0.6	ND	1.2
4	1.1	0.6	1.0	0.5	1.1	1.3
5	1.1	0.9	1.4	1.1	1.0	0.7
6	1.1	0.8	0.8	0.3	1.0	1.9
7	1.2	ND	0.8	0.8	ND	1.4
8	1.0	1.1	1.9	4.3	1.0	0.2
9	1.1	1.6	1.3	0.6	0.7	1.0
10	1.0	1.0	0.8	ND	1.0	ND
GeoMean	0.9	0.9	1.1	0.9	1.0	0.9
90% CI[a]	0.7–1.2	0.7-1.2	0.9–1.3	0.5-1.5	0.9-1.2	0.6-1.4

Abbreviations: AUCR, area under the plasma concentration-time curve ratio; CI, confidence interval; CYP3A4, cytochrome P450 3A4; GeoMean, geometric mean; ND, Not determined; sEVs, small extracellular vesicles.

[a]The sEV data supporting the determination of fold-changes are presented in Table S1. Data above are presented as the geometric mean (90% CI).

[b]Midazolam 1′-hydroxylase activity.

[c]See the Supplementary Methods in Data S1 for the prediction of midazolam AUCR ($AUC_{+PF\text{-}06835919}/AUC_{-PF\text{-}06835919}$).

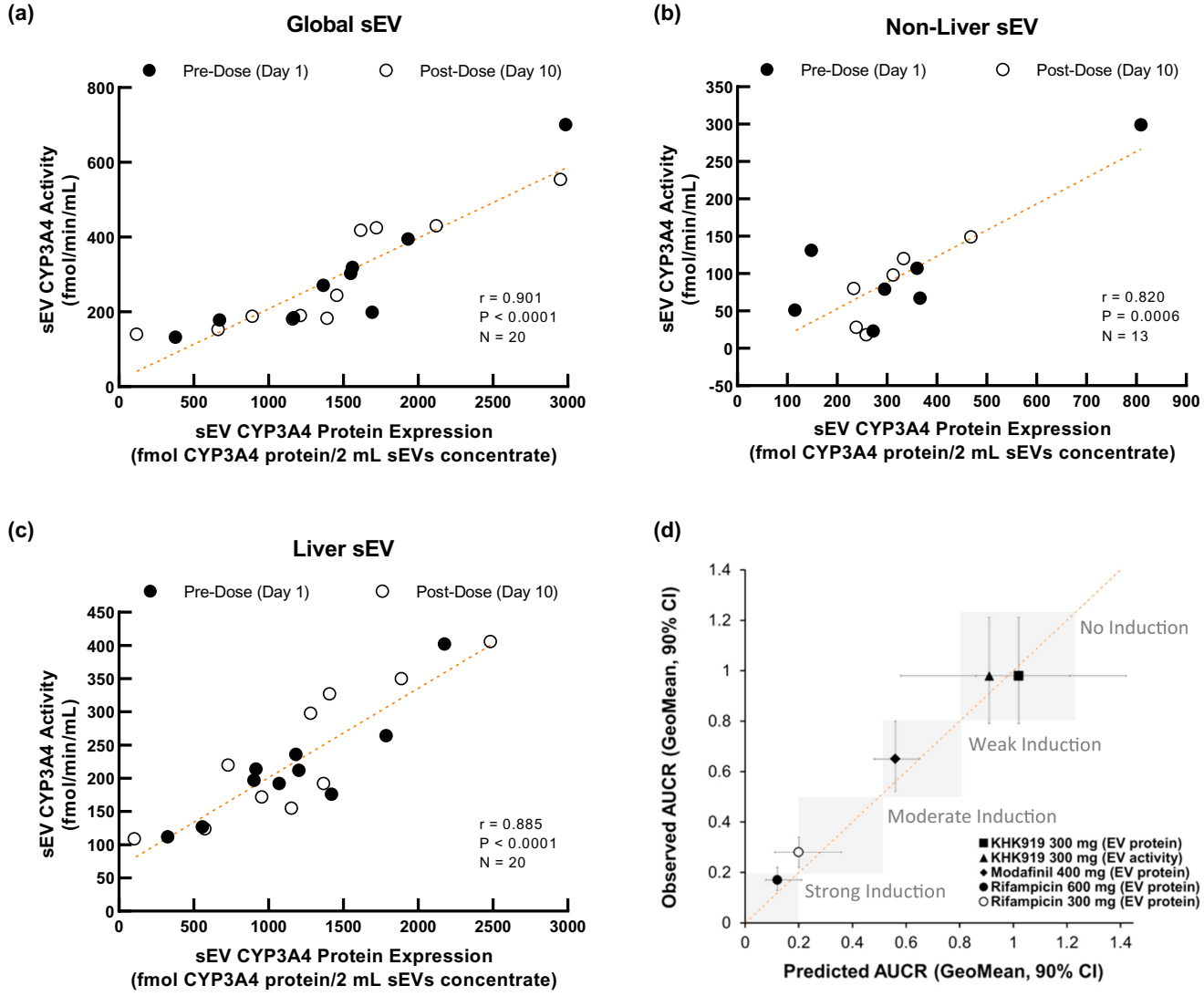

FIGURE 3 Correlation of global (a), non-liver (b), and liver (c) sEV CYP3A4 protein expression with sEVs midazolam 1′-hydroxylase activity pre- and post-PF-06835919 administration. Predictions of midazolam AUCR, based on fold-changes in sEV CYP3A4 protein expression and sEV midazolam 1′-hydroxylase activity, are also shown for PF-06835919 (d). For comparison, published data for strong (rifampicin 600 mg), moderate (rifampicin 300 mg), and weak (modafinil 400 mg) induction are shown.[12,13] AUCR, area under the midazolam plasma concentration-time curve ratio ($AUC_{+inducer}/AUC_{-reference}$); CI, confidence interval; CYP3A4, cytochrome P450 3A4; EV, extracellular vesicle; GeoMean, geometric mean; sEVs, small extracellular vesicles.

relative to midazolam administered alone, was 97.6% (79.9%–119%) and 98.9% (76.4%–128%), respectively (Table 3). PF-06835919, therefore, is not an inducer of CYP3A in vivo.

There are many possible explanations for such a discrepancy, because in vitro-to-in vivo extrapolations for the induction of enzymes, such as CYP3A4 are complex. This is especially evident when using positive in vitro hepatocyte data to predict the impact on the PK of a drug such as midazolam that undergoes both gut and liver metabolism. Such extrapolations usually necessitate the use of multi-donor preparations of qualified human primary hepatocytes, careful assessment of induction (mRNA, protein, or activity), dose dependency in vitro, generation of induction parameters, and their input into static or physiologically based PK models.[15–20] It is acknowledged that many gaps exist, including the lack of validated human primary enterocyte models to study induction, as well as robust methods to estimate the concentration of inducer in target cells, such as enterocytes and hepatocytes. This is a major challenge for sponsors of new chemical entities prior to first-in-human dosing. Because conventional pinch and needle biopsy approaches are not a viable option for routine phase I studies, some investigators deploy biomarkers, such as plasma 4β-hydroxycholesterol/cholesterol ratio and

urine 6β-hydroxycortisol/cortisol ratio, in their phase I trials.[21–24] But even such biomarkers do not provide information related to the induction of CYP3A4 in the gut versus the liver. This is especially important if new chemical entities differentially induce gut versus liver CYP3A4, as has been described for rifampicin, modafinil, and efavirenz.[13,14,25]

sEVs are small, nonreplicating, lipid-encapsulated particles that contain a myriad of protein and nucleic acid cargo derived from their tissue of origin. The potential utility of sEV-derived biomarkers to the study of drug metabolism and disposition has gained attention in recent years.[11] The key trait that makes sEVs an attractive biomarker source is their capacity to provide comparable insights to solid organ biopsy through an appreciably less invasive collection procedure. More recently, CYP3A4 induction has been studied using tissue-specific plasma (serum)-derived sEVs.[12–14] In these studies, CYP3A4 protein expression was quantitated in global (all tissues) and liver-derived sEVs isolated from the banked plasma of individual subjects dosed with CYP3A4 known inducers (rifampicin or modafinil). Moreover, it was possible to deduce the impact on non-liver (global minus liver) sEV CYP3A4 expression and activity. The individual subject sEV CYP3A4 proteomic data were used successfully to predict the exposure changes (AUCR) for different CYP3A4 victim drugs following rifampicin or modafinil. Importantly, weak to moderate inducers (i.e., modafinil) can be differentiated from strong inducers (i.e., rifampicin) using the approach.

In the current study, plasma-derived sEVs were prepared ad hoc from banked plasma for each individual subject and deployed to further assess CYP3A4 induction. As described in Figure 3, sEV-mediated midazolam 1′-hydroxylation was well-correlated with CYP3A4 protein expression across the different subjects, both of which confirmed that PF-06835919 is not a CYP3A4 inducer. Moreover, the sEV data successfully predicted the midazolam AUCR and classified PF-06835919 as a non-inducer versus modafinil and rifampicin (Figure 3d). This was plausible because midazolam is not a substrate of inducible gut transporters (e.g., P-glycoprotein or breast cancer resistance protein), is extensively metabolized by CYP3A4, and has a well-defined $f_{mCYP3A4}$ and f_g signature.[13,14,25] Such data indicate that the sEV-based liquid biopsy approach has utility in support of in vivo CYP3A4 induction assessment. Of note, the successful prediction of clinical outcomes was achieved with a simple static model (Supplementary Methods in Data S1) that did not require the input of in vitro-derived induction parameters or knowledge of PF-06835919 exposure (e.g., measured plasma concentration or estimated gut and liver concentration). In the case of PF-06835919, therefore, it was possible to address more challenging static model-based in vitro-to-in vivo extrapolations (Table 1) and help identify it as a false-positive inducer.

In conclusion, despite in vitro hepatocyte studies that suggested the potential for PF-06835919 to induce CYP3A4 at clinical doses, the present clinical study showed that with repeated dosing, the compound had a minimal effect on midazolam exposure, indicating that it is not a CYP3A4 inducer in vivo. This result was confirmed with CYP3A4 protein expression and activity assessment in the global and liver plasma-derived sEVs, which were isolated from remnant plasma samples of individual participants in the study. Plasma-derived global and liver sEVs could be a very useful tool to evaluate CYP3A4 induction in early clinical development, as it is possible to adequately quantitate protein expression in the sEVs and use the proteomic data to predict CYP3A probe drug exposure changes (AUCR) and differentiate none, weak, moderate, and stronger inducers. It is envisioned that the plasma sEV-based liquid biopsy approach could be deployed jointly with biomarkers to greatly facilitate CYP3A induction assessment in standard phase I multiple ascending dose studies. It has already been shown that changes in liver and non-liver sEV CYP3A4 expression can be used to predict changes in plasma 4β-hydroxycholesterol.[14] Therefore, an integrated sEV and biomarker dataset could be generated to de-risk CYP3A induction, circumvent the need for formal probe-based DDI studies, support the evaluation of dose-dependent induction, and, most importantly, address complex and problematic in vitro-to-in vivo extrapolations.

AUTHOR CONTRIBUTIONS

R.Q., K.F., A.D.R., J.L., M.V., D.T., A.B., and A.R. wrote the manuscript. R.Q., K.F., A.D.R., M.V., D.T., and A.B. designed the research. A.R., J.L., K.F., L.N., R.Q., D.T., A.F., A.R., and A.D.R. performed the research. A.R., L.N., Z.U., A.F., K.F, J.L., R.Q., D.T., and A.D.R. analyzed the data. A.R., L.N., Z.U., and A.F. contributed new reagents.

ACKNOWLEDGMENTS

The authors thank the Pfizer Inc colleagues Chester Costales (sEV data analysis and compilation) and Donal Gorman (statistical analysis and audit). Editorial support, under the direction of the authors, was provided by CMC Connect, a division of IPG Health Medical Communications, funded by Pfizer Inc, in accordance with Good Publication Practice (GPP 2022) guidelines.[26]

FUNDING INFORMATION

These trials were sponsored by Pfizer Inc.

CONFLICT OF INTEREST STATEMENT

R.Q., K.F., A.B., J.L., D.T., M.V., and D.R. are employees of Pfizer Inc. L.N., A.F., Z.U., and A.R. declare no conflict of interest.

DATA AVAILABILITY STATEMENT

Upon request, and subject to review, Pfizer will provide the data that support the findings of this study. Subject to certain criteria, conditions, and exceptions, Pfizer may also provide access to the related individual de-identified participant data. See https://www.pfizer.com/science/clinical-trials/trial-data-and-results for more information.

ORCID

Ruolun Qiu https://orcid.org/0000-0002-4051-6680
David Tess https://orcid.org/0000-0001-5843-7959
Lauren Newman https://orcid.org/0000-0003-3303-1666
Zivile Useckaite https://orcid.org/0000-0002-4566-5036
Andrew Rowland https://orcid.org/0000-0002-8946-3954

REFERENCES

1. Abdelmalek MF, Suzuki A, Guy C, et al. Increased fructose consumption is associated with fibrosis severity in patients with nonalcoholic fatty liver disease. *Hepatology*. 2010;51:1961-1971.
2. Abid A, Taha O, Nseir W, Farah R, Grosovski M, Assy N. Soft drink consumption is associated with fatty liver disease independent of metabolic syndrome. *J Hepatol*. 2009;51:918-924.
3. Schulze MB, Manson JE, Ludwig DS, et al. Sugar-sweetened beverages, weight gain, and incidence of type 2 diabetes in young and middle-aged women. *JAMA*. 2004;292:927-934.
4. Hannou SA, Haslam DE, McKeown NM, Herman MA. Fructose metabolism and metabolic disease. *J Clin Invest*. 2018;128:545-555.
5. Shepherd EL, Saborano R, Northall E, et al. Ketohexokinase inhibition improves NASH by reducing fructose-induced steatosis and fibrogenesis. *JHEP Rep*. 2020;3:100217.
6. Futatsugi K, Smith AC, Tu M, et al. Discovery of PF-06835919: a potent inhibitor of ketohexokinase (KHK) for the treatment of metabolic disorders driven by the overconsumption of fructose. *J Med Chem*. 2020;63:13546-13560.
7. Gutierrez JA, Liu W, Perez S, et al. Pharmacologic inhibition of ketohexokinase prevents fructose-induced metabolic dysfunction. *Mol Metab*. 2021;48:101196.
8. Kazierad DJ, Chidsey K, Somayaji VR, Bergman AJ, Birnbaum MJ, Calle RA. Inhibition of ketohexokinase in adults with NAFLD reduces liver fat and inflammatory markers: a randomized phase 2 trial. *Med*. 2021;2:800.e3-813.e3.
9. Weng Y, Fonseca KR, Bi YA, et al. Transporter-enzyme interplay in the pharmacokinetics of PF-06835919, a first-in-class ketohexokinase inhibitor for metabolic disorders and non-alcoholic fatty liver disease. *Drug Metab Dispos*. 2022;50(9):1312-1321.
10. U.S. Food & Drug Administration. In vitro drug interaction studies — cytochrome P450 enzyme- and transporter-mediated drug interactions guidance for industry. 2020. Accessed October 6, 2022. https://www.fda.gov/media/134582/download
11. Useckaite Z, Rodrigues AD, Hopkins AM, et al. Role of extracellular vesicle-derived biomarkers in drug metabolism and disposition. *Drug Metab Dispos*. 2021;49:961-971.
12. Rowland A, Ruanglertboon W, van Dyk M, et al. Plasma extracellular nanovesicle (exosome)-derived biomarkers for drug metabolism pathways: a novel approach to characterize variability in drug exposure. *Br J Clin Pharmacol*. 2019;85:216-226.
13. Rodrigues AD, van Dyk M, Sorich MJ, et al. Exploring the use of serum-derived small extracellular vesicles as liquid biopsy to study the induction of hepatic cytochromes P450 and organic anion transporting polypeptides. *Clin Pharmacol Ther*. 2021;110:248-258.
14. Rodrigues AD, Wood LS, Vourvahis M, Rowland A. Leveraging human plasma-derived small extracellular vesicles as liquid biopsy to study the induction of cytochrome P450 3A4 by modafinil. *Clin Pharmacol Ther*. 2022;111:425-434.
15. Savaryn JP, Sun J, Ma J, Jenkins GJ, Stresser DM. Broad application of CYP3A4 liquid chromatography-mass spectrometry protein quantification in hepatocyte cytochrome P450 induction assays identifies nonuniformity in mRNA and protein induction responses. *Drug Metab Dispos*. 2022;50:105-113.
16. Fahmi OA, Hurst S, Plowchalk D, et al. Comparison of different algorithms for predicting clinical drug-drug interactions, based on the use of CYP3A4 in vitro data: predictions of compounds as precipitants of interaction. *Drug Metab Dispos*. 2009;37:1658-1666.
17. Baneyx G, Parrott N, Meille C, Iliadis A, Lave T. Physiologically based pharmacokinetic modeling of CYP3A4 induction by rifampicin in human: influence of time between substrate and inducer administration. *Eur J Pharm Sci*. 2014;56:1-15.
18. Hariparsad N, Ramsden D, Taskar K, et al. Current practices, gap analysis, and proposed workflows for PBPK modeling of cytochrome P450 induction: an industry perspective. *Clin Pharmacol Ther*. 2022;112:770-781.
19. Einolf HJ, Chen L, Fahmi OA, et al. Evaluation of various static and dynamic modeling methods to predict clinical CYP3A induction using in vitro CYP3A4 mRNA induction data. *Clin Pharmacol Ther*. 2014;95:179-188.
20. Almond LM, Mukadam S, Gardner I, et al. Prediction of drug-drug interactions arising from CYP3A induction using a physiologically based dynamic model. *Drug Metab Dispos*. 2016;44:821-832.
21. Rodrigues AD, Rowland A. Profiling of drug-metabolizing enzymes and transporters in human tissue biopsy samples: a review of the literature. *J Pharmacol Exp Ther*. 2020;372:308-319.
22. Jones BC, Rollison H, Johansson S, et al. Managing the risk of CYP3A induction in drug development: a strategic approach. *Drug Metab Dispos*. 2017;45:35-41.
23. Penzak SR, Rojas-Fernandez C. 4beta-hydroxycholesterol as an endogenous biomarker for CYP3A activity: literature review and critical evaluation. *J Clin Pharmacol*. 2019;59:611-624.
24. Lee J, Yoon SH, Yi S, et al. Quantitative prediction of hepatic CYP3A activity using endogenous markers in healthy subjects

after administration of CYP3A inhibitors or inducers. *Drug Metab Pharmacokinet*. 2019;34:247-252.
25. Mouly S, Lown KS, Kornhauser D, et al. Hepatic but not intestinal CYP3A4 displays dose-dependent induction by efavirenz in humans. *Clin Pharmacol Ther*. 2002;72:1-9.
26. DeTora LM, Toroser D, Sykes A, et al. Good Publication Practice (GPP) guidelines for company-sponsored biomedical research: 2022 update. *Ann Intern Med*. 2022;175(9):1298-1304.

SUPPORTING INFORMATION

Additional supporting information can be found online in the Supporting Information section at the end of this article.

How to cite this article: Qiu R, Fonseca K, Bergman A, et al. Study of the ketohexokinase inhibitor PF-06835919 as a clinical cytochrome P450 3A inducer: Integrated use of oral midazolam and liquid biopsy. *Clin Transl Sci*. 2024;17:e13644. doi:10.1111/cts.13644